Proceedings of the 2005 IEEE/ASME
International Conference on Advanced Intelligent Mechatronics
Monterey, California, USA, 24-28 July, 2005

A New Endoscopic Microcapsule Robot using Beetle Inspired Microfibrillar Adhesives

Eugene Cheung, Mustafa Emre Karagozler, Sukho Park, Byungkyu Kim, and Metin Sitti

Abstract— **The diagnosis of gastrointestinal diseases within the small intestine has been greatly advanced with the introduction of the endoscopic microcapsule in recent years. In an effort to increase its reliability and expand its functionality, a mechanism for stopping and locomoting the capsule within the digestive tract is proposed in this paper. This mechanism, actuated by shape memory alloy wires, utilizes a synthetic microfibrillar adhesive similar to the attachment mechanisms employed by beetles. This fibrillar attachment mechanism is a combination of molecular adhesion caused by van der Waals forces and liquid adhesion caused by capillary forces. The molecular adhesion is enhanced by the presence of microfibers, and the liquid adhesion arises from a secretion from the beetle's footpad. A synthetic version of the beetle's footpad was fabricated from PDMS using a silicon mold. Another version was created from SU-8 using photolithography. Testing revealed decent adhesion with glass and prepared pig intestine *in vitro* both with a silicone oil to simulate the secretion and without it. A prototype robot with simple polymer adhesive pads for stopping successfully attached and detached inside a flexible vinyl tube. An inchworm locomotion mechanism is proposed and is in the preliminary stages of fabrication and testing.**

I. INTRODUCTION

Endoscopic microcapsules were invented as an alternative to wired endoscopes in 2001 and are now commercially available and FDA-approved for screening of the digestive tract [1]. The device resembles a large pill, and is swallowed by the patient. It navigates through the digestive tract, recording images of the tract along its journey.

There are several factors that make microcapsules advantageous to standard endoscopes. With no physical link to systems outside the body, the microcapsule is much less invasive. This also results in fewer responsibilities for the attending doctor, lowering health care costs. In addition, the microcapsule allows for *in situ* viewing of the digestive tract. Standard endoscopies require the inspected area to be cleaned and then inflated with air to facilitate passage of the endoscope. Perhaps the most important advantage is that the microcapsule can access and image the small intestine, an area of the digestive tract outside of the range of an endoscope. Despite these advantages, however, microcapsules only have an approximate fifty percent success rate for detecting diseased areas. This low percentage is due to the lack of direct control over its position, orientation and speed. Its motion is dictated by the natural peristaltic motion of the digestive tract. This project aims to provide a level of control to the microcapsule by means of a biomimetic attachment mechanism that would allow the capsule to anchor itself in one position within the digestive tract. Besides increasing the microcapsule's effectiveness in detecting diseases, attachment allows for various other capabilities in addition to imaging such as biopsies and targeted drug delivery.

Eugene Cheung is with the NanoRobotics Lab and the Department of Mechanical Engineering, Carnegie Mellon University, Pittsburgh, PA 15213, USA - eccheung@cmu.edu

Mustafa Emre Karagozler is with the NanoRobotics Lab and the Department of Electrical & Computer Engineering, Carnegie Mellon University, Pittsburgh, PA 15213, USA - mkaragoz@andrew.cmu.edu

Sukho Park and Byungkyu Kim are Senior Research Scientists at the Intelligent Microsystem Center, Korea Institute of Science & Technology, Seoul 136-791, Korea - shpark@kist.re.kr and bkim@kist.re.kr

Metin Sitti is the director of the NanoRobotics Lab and an Assistant Professor with the Department of Mechanical Engineering and Robotics Institute, Carnegie Mellon University, Pittsburgh, PA 15213, USA - sitti@cmu.edu

II. PROBLEM DEFINITION

The main challenges in the development of an attachment mechanism for a microcapsule robot are:

- Since the size of the capsule is very important (very large pills are uncomfortable), the mechanism must be sufficiently small as to not drastically increase the size of the system.
- *In situ*, the microcapsule is subject to the peristaltic motion of the digestive tract at all times – introducing the many problems of attempting to attach in a continuously moving environment.
- The attachment mechanism must be supplied with the same power that is already onboard the microcapsule. As these power systems are the limiting factor in the endurance of most capsule systems, the attachment mechanism must be low power.
- When operating within the human body, safety is a major concern – any attachment mechanism must be chosen with safety and biocompatibility as a priority.

With these constraints in mind, many traditional attachment mechanisms can be discarded. Mechanical interlocking mechanisms must not be used to avoid damaging the digestive tract. Suction based systems require too much power to be useful. Therefore, biomimetic fibrillar attachment mechanisms are selected for this research.

III. BEETLE ADHESIVE

When it comes to adhering temporarily to smooth surfaces, beetles are the undisputed champions of the natural world. One blue beetle, *Hemishpaerota cyanea*, has been found to be capable of withstanding forces of more than two hundred times its body weight for short periods (less than two minutes) of time with little energy expenditure [2]. As such, much research has been put into understanding the adhesive

0-7803-9046-6/05/$20.00 ©2005 IEEE.

mechanism employed by beetles and using this knowledge to fabricate a synthetic adhesive.

To determine the source of the beetle's adhesive strength, a simple observation of its foot pads can be extremely helpful. The feet of *Hemishpaerota cyanea* are covered with branched fibers [2]; such hairy feet are reminiscent of those seen in geckos [3], where molecular adhesion is the attachment mechanism. Molecular adhesion is based on the relatively weak van der Waals molecular attractive force. The setae of geckos are compliant structures, allowing the tips to conform to the surface. This conformation results in the setae tips getting close enough to the surface – within a few angstroms – that the van der Waals force becomes significant. When summed up over the millions of setae, the tiny molecular force becomes a macroscopic total force capable of supporting the gecko's weight [3][4].

Further observation reveals liquid droplets on the surfaces to which a beetle recently adhered [2]. Beetles secrete what is generally accepted to be a hydrophobic liquid [5] (or at least mostly hydrophobic [6][7]). This liquid, stored in some sort of reservoir within the insect, is released through tiny pores when pressure is applied to the foot. It has been found that the pores can be either at the base of the fibers [2] or at the distal ends with channels running through the setae [8]. In the case of the basal pores, it has been theorized that the liquid is drawn to the tips of the hairs in "channels" created between clumped setae [2]. The liquid secretions cause adhesion through capillary forces – forces that arise as a result of surface tension.

A. Adhesive Modeling

To further understand what roles the fibers and liquid play in beetle adhesion, a MATLAB® model was developed. The fibers were treated as oriented cylindrical cantilever beams with hemispherical tips coated with a thin layer of liquid (see Fig. 1), which is a reasonable representation of the real hairs.

The first case examined just the contribution of the fibers to adhesion, including the effects of surface roughness, fiber geometry (diameter and length), fiber density, fiber orientation, and elastic modulus [9]. Dry fiber adhesion is dominated by molecular attraction caused by the van der Waals force, which for the assumed model (a sphere-surface interaction) is given by [10]:

$$F_{vdW} = \frac{A_{12}R}{6D^2}, \tag{1}$$

where A_{12} is the Hamaker constant between fiber material 1 and surface material 2, R is the radius of the sphere, and D is the distance between surfaces (with a theoretical minimum of the atomic gap distance, D_0 = 0.165 nm). Since the total adhesion force per unit area (P_T) depends linearly on the density of the fibers (Δ):

$$P_T = F_{vdW} * \Delta, \tag{2}$$

it is clear that increasing the fiber density will result in a higher adhesive force. However, if the fibers are too dense, neighboring fibers will attract each other, possibly resulting in entanglement. The following restriction on fiber spacing was found by Glassmaker et al. to avoid this lateral collapse [11]:

$$2w > \left[\frac{L^4\gamma_s}{3Ea^3}\left(\frac{2^{11}\gamma_s\left(1-\nu^2\right)}{\pi^4 Ea}\right)^{1/3}\right]^{1/2}. \tag{3}$$

In this equation, $2w$ is the spacing between adjacent fibers, a is the fiber radius, L is the length, γ_s is the surface energy, E is the elastic modulus, and ν is the Poisson ratio (all properties of the fiber material).

For this model the fibers were assumed to be made of the polymer polydimethylsiloxane (PDMS) with Hamaker constant $A_{11} = 4.5 \times 10^{-20}$ J, and the surface material was glass with Hamaker constant $A_{22} = 6.3 \times 10^{-20}$ J. Using this matting condition to find a theoretical maximum density for a given fiber geometry, the following results from this dry adhesion model were obtained [9]:

- Thinner fibers (down to 100 nm radius) with high elastic modulus can be packed very closely together, increasing adhesion (see Fig. 2).
- Longer length and greater fiber angle increase rough surface adaptability.
- Rough surface adaptability increases adhesion due to an increased number of fibers in contact with the surface.

The second part of the model examined the effect of the secreted liquid. The adhesion force caused by a liquid bridge between a sphere and flat surface of the same material is given by [12]:

$$F_{liquid} = -\pi x_p^2 \Delta p + 2\pi x_p \gamma_L \sin\left(\theta + \theta_s\right), \tag{4}$$

where x_p is the radius of the contact line between the sphere and the liquid, Δp is the pressure difference across the free

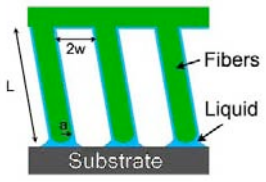

Fig. 1. Fibers were modeled as oriented, evenly spaced cylindrical cantilever beams with hemispherical tips covered in a thin layer of liquid.

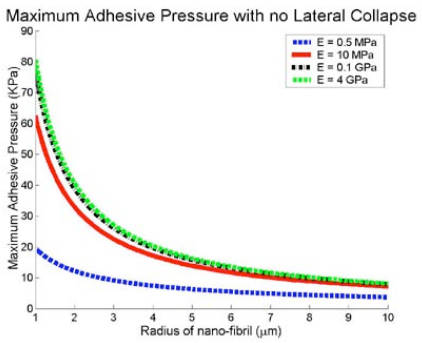

Fig. 2. Maximum adhesive pressure as a function fiber radius using the lateral collapse condition and van der Waals force model.

surface of the liquid bridge, γ_L is the surface tension of the liquid, θ is the contact angle between the liquid and solid, and θ_s relates to the slope of the sphere surface at the contact line. The pressure drop Δp is found using the Young-Laplace equation and is given by:

$$\Delta p = \gamma_L \left(\frac{1}{x_p} - \frac{1}{r} \right), \tag{5}$$

where r is the radius of curvature of the liquid bridge. For these models, it was also assumed that the fiber and surface were at the theoretical minimum separation distance of D_0 = 0.165 nm.

This liquid adhesion force was substituted for the van der Waals force in the MATLAB® model. Since A_{11} for PDMS and A_{22} for glass are very similar, the assumption that the two interacting solid surfaces are the same material is valid. The liquid used in the model was a silicone oil with $\gamma_L = 21$ mN/m and $\theta \approx 15°$, chosen for its hydrophobicity and small contact angle. The non-matting condition was applied in this model as well, with a simple substitution of $F_{liquid}/(4\pi a)$ for γ_s in 3. As can be seen in Fig. 3, the results from the two models are of the same order of magnitude, though capillary adhesion appears to provide slightly less attachment force.

B. Model Discussion

One reason that the capillary forces do not seem to be an improvement over van der Waals forces is the low surface tension of the silicone oil (compare with $\gamma_L = 72.8$ mN/m for water). It has been suggested that the beetle's secretion is not purely hydrophobic, but rather an emulsion of volatile hydrophilic droplets within a hydrophobic base [6][7]. This may be to get the benefits of both the low contact angle of the hydrophobic base and the high surface tension of the hydrophilic droplets. Further investigation is needed to confirm this hypothesis.

While the capillary forces alone may not be sufficient to account for the strength of beetle adhesion, the fibers within the liquid will still exhibit some solid-solid interaction with the surface. Thus, when considering the total attractive force between a sphere and surface, molecular attraction between the solids must also be included. Assuming that only dispersion forces are responsible for any interaction, the solid-solid attractive force inside the liquid bridge is given by [10]:

$$F_{SS} = 4\pi R \gamma_{SL}, \tag{6}$$

$$\gamma_{SL} \approx \gamma_S + \gamma_L - 2\sqrt{\gamma_S^d \gamma_L^d}, \tag{7}$$

where γ_{SL} is the interfacial surface energy between the solid and liquid, γ_S is the solid surface energy (related to the Hamaker constant by the equation $A_{11} = 24\pi\gamma^d D_0^2$ [10]), and γ^d is the dispersion force contribution to surface energy.

Another factor to be considered is friction within the liquid. Pulling the fiber off of the surface results in liquid shearing due to viscosity. Using a simple parallel plate model with a Newtonian liquid, this viscous drag force is given by [6]:

$$F_\eta = \frac{Av\eta}{h}, \tag{8}$$

where A is the area of the plate, v is the velocity of plate separation, η is the viscosity of the liquid, and h is the initial plate separation distance.

An important factor not included in the capillary adhesion model is rough surface adaptation. Liquid can fill in or smooth over pits or asperities that would otherwise inhibit dry adhesion.

IV. ADHESIVE FABRICATION

The NanoRobotics Laboratory at Carnegie Mellon University has become proficient in the fabrication of high aspect ratio fibers with diameter on the length scale of one micron [13][14]. The latest fabrication technique involves creating a mold using deep reactive ion etching of a silicon wafer. After a passivation step to aid release, polymers such as PDMS and polyurethane (WC781, BJB Inc.) are poured onto the mold and mechanically removed upon curing. As can be seen in Fig. 4, this process yields very reliable high aspect ratio fibers.

Another technique that we are currently developing involves the use of the photoresist SU-8 as the fiber material. This enables fiber fabrication with just UV exposure through a mask, as well as the creation of more complicated structures, such as a method for effecting liquid secretion. The design calls for the passive pressure applied by the foot upon contacting the ground to push liquid from a chamber in the foot through pores on the footpad. First, a layer of Omnicoat (from MicroChem Corp.) is spun on a silicon wafer for release, and then a layer of SU-8 is spun on with the desired

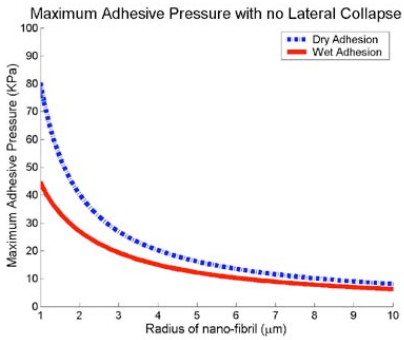

Fig. 3. Comparison of the dry adhesion (van der Waals) model with the wet adhesion (capillary) model. While the same order of magnitude, capillary adhesion model results in a smaller attachment force.

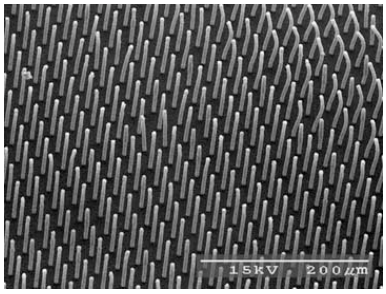

Fig. 4. Array of 4μm diameter molded polyurethane fibers.

thickness for the backing layer of the fibers. The desired pore pattern is exposed on the SU-8 and then etched, resulting in an SU-8 layer with pores. Another layer of SU-8 is deposited with a thickness that is the desired length of the fibers, which is then exposed with the desired fiber pattern and etched. Any fibers that overlap with pores will be released in the etching, leaving the pores unobstructed. The final step is to etch away the Omnicoat to release the SU-8 membrane from the silicon wafer.

A. Characterization System

Once the fibers are fabricated, their adhesive strength must be characterized. To accomplish this task, a custom force measurement system was set up using an automated stage, cantilever beam, and some simple electronics (Fig. 5). The deflection of the cantilever beam is measured using two strain gages (ESB-20-350; Entran Devices, Inc.) placed in a Wheatstone bridge circuit. The output voltage is amplified and fed into a data acquisition board. The computer software reads the voltage, calculates the force on the beam, and outputs commands to move the stage accordingly. Since noise becomes a significant problem in the cantilever setup for forces less than 50 mN, a ten gram load cell (GSO-10; Transducer Techniques Inc.) can be used instead of the beam to allow for higher resolution measurements of small forces.

The surface to which the samples adhere to is a glass slide attached to the end of the cantilever beam or load cell. If another surface is desired it can be affixed to the glass slide. The adhesive sample is attached to a sample holder on the automated stage. This holder is currently a rigid surface attached to a flexible suction cup (B10-2.20.01AC; RA Hiller Co.) to reduce alignment errors. To take a measurement, the stage moves the sample toward the glass slide at a preset approach velocity. When the applied force reaches the desired preload value, the stage stops and the sample remains in contact with the surface for a preset amount of time. Finally, the sample is moved away from the slide with a preset retraction velocity. The adhesion force is the maximum measured force while the sample is being pulled away from the surface.

Tests were also run to examine the effects of a liquid film on adhesion. The liquid used was a silicone oil from Dow Corning with 350 centistoke viscosity. To control the thickness of the liquid film, the silicone oil was spun onto the sample at 4000 RPM for a duration of 30 seconds unless otherwise noted.

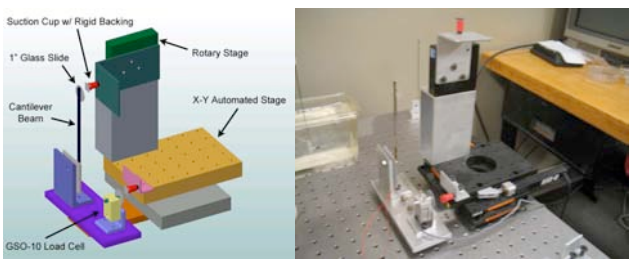

Fig. 5. On the left is the SolidWorks model of the force measurement system. The right image is a photo of the built system.

B. PDMS Characterization

PDMS is a sticky, soft polymer that was one of the first polymers in which the NanoRobotics lab was able to obtain uniform well-structured fibers. Being also very simple to fabricate, the first characterization efforts were focused on this material. Initial tests probed the effect of preload and stage speed on adhesion. For all of these initial tests the contact time was fixed at 2500 ms.

The first tests were done with flat PDMS on glass. Dry flat PDMS exhibited strong adhesion with glass; the maximum measured adhesion force of 12.9 kPa using a 20 kPa preload was only one order of magnitude less than the adhesion seen in geckos. As expected, greater preload forces resulted in stronger adhesion from greater roughness adaptation. Increased stage velocity also tended to increase adhesion due to the viscoelastic properties of PDMS. The samples with spun on silicone oil exhibited good adhesion as well, although not as strong as the dry samples. The increased adhesion in the dry samples can be attributed to an additional surface interaction between the PDMS and the glass slide (likely hydrogen bonding) that was not present when liquid is introduced.

The next set of tests were with molded PDMS fibers (4 μm in diameter and spaced 18 μm apart center-to-center) on glass. One would expect that PDMS with molded fibers would result in less adhesion simply due to less surface area in contact. However, the test results showed a significant reduction in adhesion to 0.6 kPa (an order of magnitude less than seen with flat PDMS). One reason for this (seen also in [15]) was the reduction in actual contact area. With the given fiber dimensions and spacing, the actual contact area has been reduced to about 4% of a perfectly flat surface. Taking this into account, the adhesion pressure for the flat surface and the 4 μm fibers were comparable. If the overall adhesion force is to be increased without the use of another agent (such as liquids for capillary adhesion), thinner fibers in higher density arrays must be used. The fiber samples with silicone oil spun on showed good adhesion, slightly higher than the wet flat PDMS samples. A maximum adhesion pressure of 13.0 kPa was measured for a 20 kPa preload. All of the general trends seen with the flat PDMS samples were also reflected in the PDMS fiber adhesion data. Increased preload and increased stage speed all resulted in greater adhesion force.

The next step in determining the feasibility of this adhesive system for use with an endoscopic microcapsule is the taking of adhesion measurements with actual intestinal tissue. For *in vitro* testing, pig intestines were purchased from the local meat butcher. The intestines were washed and cut so that a single layer could be affixed to the glass slide. All of the same tests that were performed with PDMS on glass were then performed with PDMS on intestine.

Flat PDMS samples showed the same trends in relation to preload and stage speed that were seen in the glass adhesion tests. Unlike glass, though, adhesion increased as expected when the silicone oil was spun onto the PDMS. When

compared to the flat PDMS samples on glass, the adhesion to intestine can be seen to be slightly less. A maximum adhesion pressure of 8.6 kPa was measured for a 20 kPa preload. This is expected since the intestine has a much higher surface roughness than glass; the flat PDMS will be unable to conform to the roughness, decreasing the amount of area in close contact resulting in less adhesion.

The test most applicable to the target application was the PDMS fiber samples on intestine (see Fig. 6). As can be seen on the graph, not only do all the expected trends regarding preload and stage speed hold, but this combination provides the largest measured adhesion of all the tests (a maximum of 18.5 kPa for a 20 kPa preload). Although at low preloads and speeds the wet samples showed less adhesion than dry, the other end of the spectrum (high preload and stage speed) had the wet tests out-perform the dry.

The effect of contact time was also tested in each of the eight adhesion types (dry or wet, flat or fiber, glass or intestine). In theory, if the sample is in contact with the substrate for a longer period of time the materials and liquids have more time to conform and fill in gaps in the interface, resulting in greater adhesion. In all cases increased contact time corresponded to increased adhesion, as expected.

Another variable of interest in the wet tests is the thickness of the liquid layer. This thickness is controlled via the spinning speed when the silicone oil is applied. While it is expected that a thinner liquid layer (and therefore higher spin speed) would increase adhesion, thus far the results have been inconclusive. Multiple runs of the same test produce the whole spectrum of results. Sometimes the adhesion stayed constant and seemed independent of spin speed, while other times the adhesion would increase or decrease. More work must be done to determine why these results vary so greatly.

These characterization results are very promising. The low density PDMS fibers showed enhanced adhesion over plain flat PDMS when sticking to pig intestines. The addition of silicone oil also resulted in increased adhesion. These benefits should become even more noticeable with superior PDMS fibers (higher density, higher aspect ratio) and possibly even a better liquid.

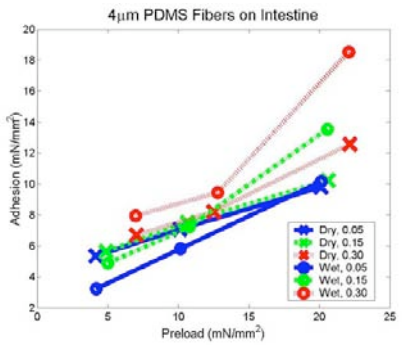

Fig. 6. Characterization results of 25 mm^2 PDMS samples with 4 μm diameter fibers showing the effects of preload and stage speed on adhesion with *in vitro* intestinal tissue. Increased preload and increased stage speed result in increased adhesion.

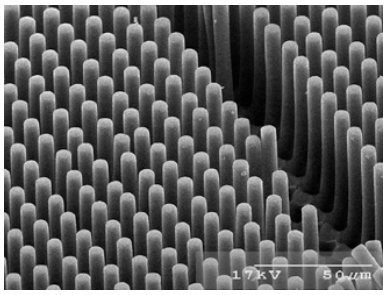

Fig. 7. SEM image of 5 μm diameter, high density, high aspect ratio fibers.

C. SU-8 Characterization

The next material to be tested was the photoresist SU-8 since a fairly simple method of fabricating integrated pores and fibers has been formulated using this material. Fabrication of high density, high aspect ratio fiber arrays has been successfully achieved (see Fig. 7) using standard SU-8 processing.

Some initial measurements have been taken using 5 μm diameter fibers, and the results are very promising. Once again, the most noteworthy combination – wet fibers on intestine – produced the most adhesion (8.5 kPa adhesion with 11 kPa preload). These values appear to be in line with the results from the PDMS tests. If the decreased stage speed and shorter contact time are taken into account, it can be inferred that the SU-8 hairs out-perform the PDMS hairs. More comprehensive testing must be completed before this can be stated with certainty.

V. CAPSULE PROTOTYPE

A. Design

Returning to the problem definition, the list of challenges in the design of an attachment mechanism also apply to the selection of the actuators. To summarize, the actuator must be safe to use inside the human body, have large strain capability, produce high output force, draw low power, and be small in size. A secondary concern is the speed of the actuator – while a fast response time would be preferable, the current goals do not require it.

Piezoelectric materials were considered for their small size, high output force, quick speed, and low power consumption. However, the need for a high driving voltage raises questions as to its biocompatibility. Combined with its small strain capability, this was determined to be reasonable cause to look at other actuators.

Polymer actuators have become increasingly popular in robotics. The large strain capability and its biocompatibility are attractive. Unfortunately, these actuators are slow, relatively bulky, incapable of high output force, and consume large amounts of power.

The next actuator considered was shape memory alloy (SMA). This type of actuator had all the qualities necessary for this device with two exceptions. SMA is heat-activated and thus fairly slow. In addition, this means that the device dissipates a lot of power. Despite this drawback, it was decided that SMA would be sufficient for the purposes of

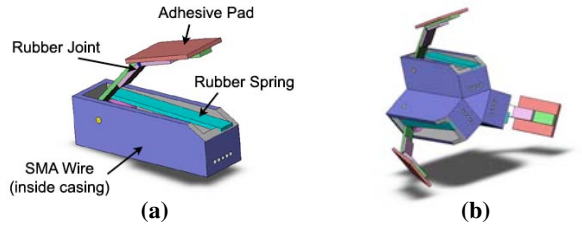

Fig. 8. SolidWorks drawings of the SMA-actuated leg design, single leg (a), and with three legs together to form the capsule prototype (b).

a tethered prototype. The issue of power consumption will be addressed as the project progresses further.

The initial stopping mechanism design calls for three "legs", one of which is shown in Fig. 8a. It is desired to rotate the leg such that the adhesive pad on the leg can be made to touch and preload the intestine walls, enabling the microcapsule to stick. The mechanism has an outer casing (blue) that mounts the rest of the parts. The adhesive pad (red) is attached at the end of the leg (green), which is made compliant with a passive polymer hinge (light purple). The entire leg structure is mounted on a cylindrical pulley (purple) that is free to turn on a pin mounted on the case. A rubber spring (turquoise) keeps the inactivated leg in the closed position. The actuator, an SMA wire, is threaded through the casing three times via holes at the front and back to achieve a longer stroke. The ends of the SMA are attached on one end to the casing and to the pulley on the other end.

When the SMA is heated by passing current through the wire, it contracts and pulls the cylindrical pulley, creating a torque. This torque rotates the pulley, thereby rotating the attached leg. The spring (rubber) is also connected from one end to the pulley, and to the casing from the other end. This rotation stretches the rubber spring, applying a torque in the opposite direction, and the leg will reach a stable point where the torques are equal. To pull the leg back to its initial position, the current through the SMA is simply shut off. The energy now stored in the spring will turn the pulley back to its original state.

The purpose of the leg compliance created by the polymer hinge is to aid the adhesive pad in sticking to and detaching from to the walls of the intestine. When the pad starts to touch the intestine wall, the leg bends, applying both shear and normal preload. Consequently, when the leg closes, this structure creates a peeling motion, greatly reducing the force necessary to detach. This compliant structure is formed using a stiff rubber, which connects two separate parts of the leg.

Three leg mechanisms will be connected together to form the complete stopping mechanism for the microcapsule (see Fig. 8b). All three legs will be actuated simultaneously for simplicity.

B. Fabrication

A prototype leg mechanism was fabricated and successfully tested. The casing, cylindrical pulley and leg were built from Delrin, which is a hard but easy to machine polystyrene. The casing is a 6mm by 6mm by 20mm rectangular box with one open face and 0.8mm thick walls. The pulley is 4.2mm wide and 3mm in diameter, and on the surface there is a groove to seat the SMA wire. The SMA used was 100μm in diameter, and the leg length is 18mm in total. The hinge was placed at 12mm, and the adhesive pad was a 3mm by 5mm by 0.5mm thick piece of PDMS. The parts were connected using loctite 414 super bonder. The external wire connections to the SMA were done using mechanical clamping.

The successful tests of the single leg led to the construction of the three legged capsule design. Two more legs were constructed as nearly identical to the first as possible and the three leg mechanisms were then glued together. The three SMA actuators were connected in series so as to reduce the total amount of current needed to be supplied. To protect against any failures, the device has held with a tether made out of green wires that prevented the capsule from free falling during tests. When a current of 180 mA (at 9.4V) was applied, the three legs extended in unison. To test its stopping capabilities, a clear vinyl tube with an inner diameter of 1 inch was obtained and set up vertically on the test bench. The capsule was then lowered into the tube with the tether and current was applied, stopping the capsule within the tube (see Fig. 9). When the current was removed, the legs retracted to their original position, peeling the adhesive pads off of the wall per the design and detaching the capsule from the walls of the tube. The capsule could then continue to be lowered down the tube, and actuation could be repeated to attach to and detach from the walls again. To ensure that it was not the tether that was supporting the capsule but the adhesive pads themselves, the tether was wiggled and even released; the prototype always held its position within the tube. In addition, the capsule prototype was tested within a larger vinyl tube with an inner diameter of 1.25 inches. The capsule performance was comparable to that in the smaller tube. These tests showed that this prototype is capable of basic stopping performance in accordance with the design parameters.

The prototype leg mechanism constructed works robustly and promises to cover the basic requirement; it appears to provide enough preload on the adhesive pads. Parameters such as spring stiffness, initial spring deflection, SMA wire type and diameter should be optimized before the more

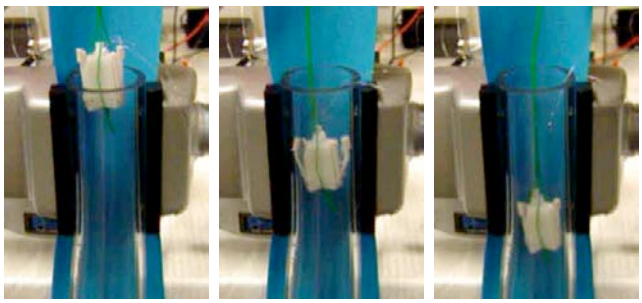

Fig. 9. Stills of a movie where the leg prototype is lowered into the vinyl tube (left), whereupon current is applied and the capsule stops itself (middle). When the current is removed, the legs retract, detaching from the walls and the capsule continues down the tube (right).

precise fabrication of a smaller prototype is completed.

Another current challenge is to increase the range (angle) of the leg mechanism. A more accurate machining/gluing process may help in avoiding misalignments and friction, thus providing for a smoother movement with a larger range.

C. Locomotion

With a feasible stopping mechanism, the device can be expanded quite simply into a locomotion mechanism. For movement inside the digestive tract, and inchworm mechanism has been found to be the most appropriate approach [16] [17]. The proposed design (see Fig. 10) is composed of two casings on which leg assemblies similar to the ones used in the stopping device are attached. The two casings slide over a hollow cylinder, forming a piston, and are connected with a spring and SMA wire. When activated, the SMA wire pulls the ends of the capsule together, compressing the spring. When the SMA is deactivated, the spring returns the capsule to its expanded rest state. Inchworm movement is achieved in the traditional manner by actuating the legs and piston in the appropriate sequence. At any time, one set of legs is always open, anchoring the capsule to the intestine walls, while the other casing is moved (either pushed or pulled).

Thus far, the locomotion mechanism has not been completely fabricated. A piston mechanism was fully constructed with an incomplete set of legs to demonstrate proof of concept. At rest, the capsule is 2.2 cm in length and 1.0 cm in diameter. Experiments show that the piston has a 5mm stroke, taking about 8 seconds for a full cycle. Therefore, the device can achieve a theoretical speed of almost 4 centimeters per minute.

VI. CONCLUSIONS AND ACKNOWLEDGEMENTS

A. Conclusions

This project demonstrates significant progress toward the development of a stopping mechanism for the endoscopic microcapsule using a synthetic beetle adhesive. A simple model has been implemented to explore various aspects of the adhesive system, revealing the important parameters for increased adhesion and rough surface adaptation. The capability to reliably fabricate high aspect ratio micro-fibers in polymers and SU-8 has been acquired. Experiments verify the adhesion contribution from a hydrophobic liquid. This force was found to increase with preload, velocity, and contact time, all agreeing with theory. A working leg prototype has been constructed, verifying the feasibility of the SMA actuated design. The project is well on the way towards the completion of a viable stopping and locomotion mechanism for the endoscopic microcapsule.

(a) **(b)**

Fig. 10. SolidWorks drawings of the proposed locomotion mechanism, a) in exploded view, and b) in the rest (expanded) state.

B. Acknowledgements

The authors gratefully acknowledge the financial support of the Intelligent Microsystem Center (www.microsystem.re.kr), Seoul, Korea, which is carrying out one of the 21st century's New Frontier R&D Projects sponsored by the Korea Ministry of Commerce, Industry & Energy. The authors would also like to thank Mike Murphy for his work on the synthetic adhesive fabrication and Gaurav Shah and Burak Aksak for their work on the adhesive model.

REFERENCES

[1] Given Imaging Ltd. http://www.givenimaging.com.
[2] T. Eisner and D. Aneshansley. Defense by foot adhesion in a beetle (*Hemisphaerota cyanea*). *Proceedings of the National Academy of Sciences*, 97(12):6568–6573, 2000.
[3] K. Autumn et al. Adhesive force of a single gecko foot-hair. *Nature*, 405:681–685, 2000.
[4] K. Autumn et al. Evidence for van der waals adhesion in gecko setae. *Proceedings of the National Academy of Sciences*, 99(19):12252–12256, 2002.
[5] A. Kosaki and R. Yamaoka. Chemical composition of footprints and cuticula lipids of three species of lady beetles. *Japanese Journal of Applied Entomology and Zoology*, 40(1):47–53, 1996.
[6] W. Federle et al. An integrative study of insect adhesion: mechanics and wet adhesion of pretarsal pads in ants. *Integrative and Comparative Biology*, 42(6):1100–1106, 2002.
[7] W. Votsch et al. Chemical composition of the attachment pad secretion of the locust *Locusta migratoria*. *Insect Biochemistry and Molecular Biology*, 32(12):1605–1613, 2002.
[8] S.N. Gorb. The design of the fly adhesive pad: distal tenent setae are adapted to the delivery of an adhesive secretion. *Proceedings of the Royal Society of London, Series B*, 265(1398):747–752, 1998.
[9] G. Shah and M. Sitti. Modeling and design of biomimetic adhesives inspired by gecko foot-hairs. In *IEEE International Conference on Robotics and Biomimetics (ROBIO)*, Shenyang, China, August 2004.
[10] J. Israelachvili. *Intermolecular & Surface Forces*. Academic Press, 1992.
[11] N.J. Glassmaker et al. Design of biomimetic fibrillar interfaces: 1. making contact. *Journal of The Royal Society, Interface*, 1(1):23–33, 2004.
[12] A. de Lazzer, M. Dreyer, and H.J. Rath. Particle-surface capillary forces. *Langmuir*, 15:4551–4559, 1999.
[13] M. Sitti and R.S. Fearing. Synthetic gecko foot-hair micro/nano-structures as dry adhesives. *Journal of Adhesion Science and Technology*, 17(8):1055–1073, 2003.
[14] C. Menon, M. Murphy, and M. Sitti. Gecko inspired surface climbing robots. In *IEEE International Conference on Robotics and Biomimetics (ROBIO)*, Shenyang, China, August 2004.
[15] C.Y. Hui et al. Design of biomimetic fibrillar interfaces: 2. mechanics of enhanced adhesion. *Journal of The Royal Society, Interface*, 1(1):35–48, 2004.
[16] P. Dario et al. Modelling and experimental validation of the locomotion of endoscopic robots in the colon. *Springer Tracts in Advanced Robotics*, 5:445–455, 2003.
[17] A. Menciassi et al. Robotic solutions and mechanisms for a semi-autonomous endoscope. In *Proceedings of the IEEE RSJ International Conference on Intelligent Robots and Systems*, Lausanne, Switzerland, October 2002.